Preliminary Validation of UWB Through-Rubble Detection Measurements for Quasi Real Time Detection of Trapped Survivors

Tareq F. A. Zanoon

Computer Systems Engineering Department.
Arab American University AAUJ
Jenin, Palestine
tareq.zanoon@aauj.edu.

***Abstract* - This paper discusses the validation of simulation data for through rubble detection through a preliminary experimental setup. The experimental feasibility of detecting body limb movements through rubble is also investigated. The setup relies on illuminating a series of UWB transceivers arranged in a C- shaped antenna array scanner in a limited view geometry where data is repetitively and continuously collected over small time intervals. Image reconstruction is based on a multi-static multilateration method which correlates the movements captured by subtracting successive signals obtained from each transmitter-receiver pair into a point on the image. Experiential measurements of the basic setup show good agreement with simulated data, and demonstrate the capability of detecting targets displaced more than 30 cm beyond concrete barriers without requiring any priori information.**

Keywords - UWB imaging; Through rubble imaging; Mutlilateration

I. INTRODUCTION

The search for survivors trapped under rubble is the top priority for search and rescue missions whenever disaster strikes. Whether natural or manmade, victims are trapped in cavities surrounded by several random layers of unstructured building materials ranging from concrete, wood, re-bars, rocks, clay, glass, and many others. The development of detection tools that can aid in search and rescue operations in the limited time window is crucial to saving lives.

Ultra-Wide Band (UWB) imaging has been previously investigated for non-invasive imaging applications, such as Ground Penetrating Radar (GPR), and medical imaging [1, 2]. Through wall imaging and sensing are among the recent emerging applications of UWB imaging, and are the focus of ongoing research that aims to target a verity of purposes [3-5]. Given the diversity and unique characteristics of these imaging applications, each area has driven its own data acquisition modalities, optimum sensor positioning, and image reconstruction algorithms.

Imaging through rubble to search for survivors requires a fast computing approach, thus excluding computationally intensive non-linear iterative reconstruction methods. Multilateration, and Synthetic Aperture Radar (SAR) techniques have been commonly used for a variety of radar applications, including through wall imaging [4, 7]. These methods are computationally cheap looking from the image reconstruction time perspective. However, they suffer from ambiguities in cases of multiple reflections. Furthermore, these approaches, in general, neglect propagation distortion encountered by signals passing through multiple layers of interfaces due to the free-space or media wave speed assumption, thus leading to ambiguities and distortion in the resulting image. For simple cases of a single wall barrier of uniform thickness and uniform permittivity, wall parameters are usually estimated, modelled, and subtracted from the measured signals. However, this approach does not apply in the case of unknown random rubble, and therefore, their application is confined within the particular area of application. The fast computing advantage of the multilateration methods can be only realized within the confined limits of the application, and cannot be generalized.

Localization of targets in through rubble detection has more priority compared to revealing full features about the surrounding structures, although the later can be of beneficial use. Imaging in such cases can be viewed based on whether information is sought on motion within a structure, or on imaging the stationary structure itself. For the application in hand, it is sufficient to detect the presence of a survivor and his proximate location without the need to reveal the features of the potential complex unknown layers of different building materials stacked at random orientations.

Several studies have been performed to filter human motion from stationary objects by means of data subtraction in order to detect changes [8]. In [9], change detection is obtained by a cross-correlation image subtraction method requiring reimaging of the same seen at two different time instances, while in [10], change detection is obtained from subtraction of the downrange over consecutive data frames. The majority of published literature on through rubble detection focuses on extracting heartbeats and breathing patterns as they can be isolated as periodic signals [11,12].

However, these approaches ignore non-periodic changes such as those obtained via limb or body movements. In comparison, limb or body movements provide a more significant response in the reflected signal in comparison with weak signals obtained from heart beat and respiration movements [13]. Other methods in literature focus on the discrepancy of dielectric constant between rubble and human tissue [14]. Such approaches however have their limitations in cases of reflective rebar, or in the presence of a none-human high dielectric media, such as spilled water, wet concrete or mud, all which are very likely to be present in cases of disasters.

To overcome such limitation, a new proposed approach was suggested [15] focusing on change detection to detect minute movements of limbs or respiration for targets trapped under uncertain amount of obstruction rubble. Change detection is computed by subtracting measurements of each transmitter-receiver pair of a multi-static sensor array obtained from two successive time frames, thus subtracting heavy clutter caused by reflection, refraction, diffraction, and dispersion of multiple stationary obstruction boundaries, leaving only the response due to movement. A multilateration method was then used to correlates the target reflections based on Time Difference of Arrival (TDOA), to a single point on the image, where reflection points start to integrate.

The primary objective in formulating the approach above was the capability of detecting any type of movement, offering results in quasi-real time without priori information, or estimation parameters. However, the study was based on data obtained via simulation for various numerical setups. In this paper, a preliminary experimental setup is used to validate the simulated data and examine the reconstruction approach using experimental data.

II. Mathematical Model

The mathematical image reconstruction approach is fully described in [15], and is repeated here for the sake of completeness. When a limited view multi-static arrangement is considered (Fig.1), measurements are obtained by illuminating the target twice by transmitter over two successive time instances at (t) and (t +1), while the remaining displaced antennas record the backscattered signals at both time instances. This process is repeated sequentially for each antenna element, thus gathering more information from the imaging scene.

Considering the m^{th} transmitter and the n^{th} receiver, the total distance between points *m*, *P*, and *n* can be expressed as:

$$R_{m,n} = a_m + b_n \tag{1}$$

where a_m is the distance between the transmitting antenna and the target *P*, while b_n is the distance from *P* to the receiver. With two successive time-domain measurements, the TDOA along the propagation path can be obtained finding the time of flight by:

$$TA_{m,n} = s_{m,n}^{t+1} - s_{m,n}^{t} \tag{2}$$

where $s_{m,n}$ is the backscattered signal at receiver *n* due to the excitation of the m^{th} transmitter at time instances *t*+1 and *t* respectively.

From a stationary perspective, $s_{m,n}^{t+1}$, and $s_{m,n}^{t}$ will be exactly identical, canceling each other completely (common signals). However, any minute variation of the assumed target, in terms of position or size, will be distinctly observed and attributed to target motion, as all effects associated with stationary obstacles will be canceled regardless of material type, size, or orientation. Thus, reflection, refraction, diffraction, as well as dispersive effects of stationary obstacles will be canceled leaving only the target response.

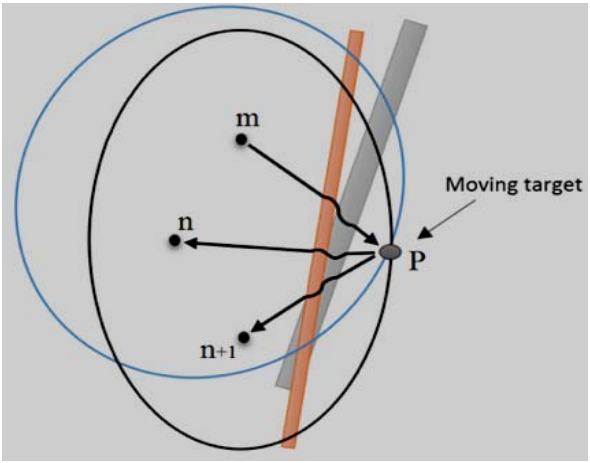

Fig. 1. Partial representation of the limited view multi-static configuration illustrating two transmitter-receiver pairs, and their corresponding ellipses.

Along the propagation path from the transmitter, the wave travels in free space until encountering the first wall/obstacle interface. Beyond the first interface, the propagation speed depends on the type of material and structure being penetrated. The same process happens in reverse on the way to the receiver.

The relative permittivity for various types of building material are around 2,2,5,8, and 4 for plywood, drywall, brick, solid concrete, and hollow concrete respectively [16], thus affecting the propagation speed. The speed of the wave propagating in random rubble beyond the first wall interface can only be speculated due to the complexity of the structure. Adding to the complication is the potential presence of partial amounts or re-bars resulting in partial reflections. To overcome this issue, the positional accuracy can be compromised in favor of fast detection capability of targets buried within the vast number of unknown variables. Bearing this in mind, and assuming free space propagation speed c, the distance travelled can be approximated as:

$$R_{m,n} = TA_{m,n} \times c \quad (3)$$

where $TA_{m,n}$ is the calculated TDOA obtained from the time domain measurements $s^{t}_{m,n}$ and $s^{t+1}_{m,n}$.

The distance $R_{m,n}$ corresponds to a constant range contour of an ellipse, which has its focal points at points *m*, and *n*. Repeating the process for the $n^{th}+1$ receiver would yield $R_{m,n+1}$which is another elliptic contour with focal points at points *m* and $n+1$. Both contours will have an intersection point at *P* at least. In a 2D rectangular coordinate system, the group of ellipses that describe the range between receivers and the m^{th} transmitter are given by:

$$R_{m,n} = \sqrt{(x_m\text{-}x)^2 + (y_m\text{-}y)^2} + \sqrt{(x_n\text{-}x)^2 + (y_n\text{-}y)^2} \quad (4)$$

where (x_m, y_m), and (x_n, y_n), define the location of the transmitter and receivers' n = 0,1, …, *N*, and (x, y) is the position location estimate of the target (intersection point). A target location can be uniquely determined by the intersection of three or more ellipses. This process is also repeated for the remaining transmitters *m* =1,2, … *M*, according to the multi-static configuration.

III. Materials & Methods

A. Nuerical Model

The numerical model is based on five UWB transceivers arranged in a multistatic configuration. For each transmitter, four measurements will be recorded resulting in an overall of 20 transmitter receiver pairs. The transceivers are arranged in a C-shape like arrangement to aid in the viewing geometry given the limited view of the problem.

A 0-1 GHz UWB impulse is used to illuminate the imaging domain. The lower frequencies allow better penetration depth within the structure under investigation, while the higher frequencies will allow detection of spatial resolution required to detect small movement variation such as respiration. Fig. 2 shows the sensor configuration and scanning position. In principle, the sensor array can be oriented to target the search area.

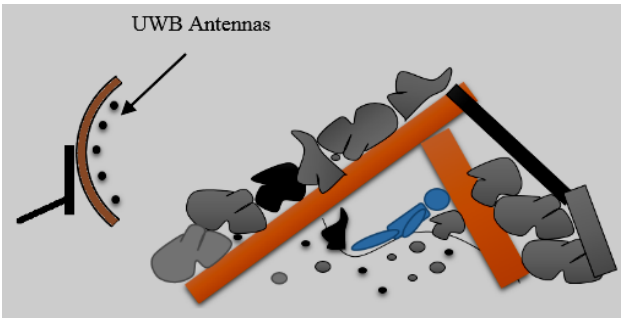

Fig. 2. Sensor configuration and scanning position.

To investigate the detection approach proposed earlier, a numerical model is set using the Finite Difference Time Domain method. The forward setup follows that described in [6]. The target detection approach is attempted on a 2-D 2m × 2m numerical domain, where the imaging space is discretized intro 100 x100 cells with a spatial step of $\Delta x = \Delta y = 2\text{cm}$, and a time step of Δt = 33.3 pS. A PML boundary region of 10 cells is established around the problem space. The permittivity of building various building materials are followed as described in [16].

B. Measurements and Data Acquisition

Measurements and data acquisition is based on a set of UWB biconical antennas, serving as sensors, and focusing on the target from a single side. The antennas are driven via a 50 Ω coaxial feeder, incorporating in-line ferrite torroids to ensure balanced antenna feeding, and through which an RG58 coaxial cable is threaded.

The data acquisition system is composed of an R&S ZVL 6 Vector network analyzer providing measurements in time domain. This acquisition system communicates with a PC to automate data capture, processes the reconstruction algorithms and displays the image. A calibration procedure is followed to account for cable lengths since they are not modeled in the simulation.

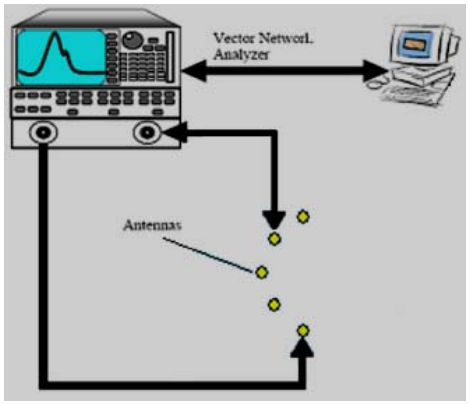

(a)

(b)

Figure 3. The experimental set-up for UWB tomography, (a) the schematic and (b) the essential elements

Concrete blocks were used to construct the main wall barrier. Each block is a hollow 10 cm thick, with air gaps, as can be observed in Fig. 3, resulting in a none-homogeneous concrete structure barrier. Water filled bottles of various sizes were used to construct a human dummy with torso & limbs.

IV. Results and Discussion

Initial validation is carried out by forming a simple experimental setup to compare experimental and simulated generated data. In this simple setup, the target is assumed to be a 5 litre water filled container initially placed 14 cm from the other side. To induce movement, the target was shifted 4cm away from the barrier. The numerical setup was modelled to follow that of the experimental setup (Fig. 4).

Figure 5 compares the data obtained from both setups for sensor 2 with respect to all receivers. Each curve is obtained by subtracting the corresponding (t+1) and (t) instances related to object movement.

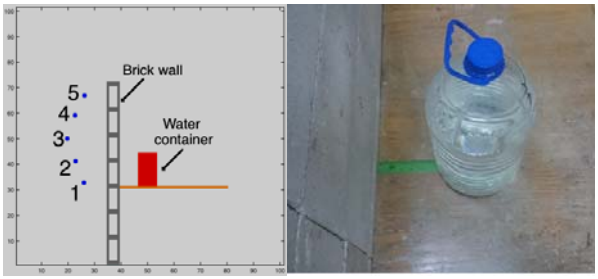

(a) (b)

Figure 4: Simple target experiment showing: (a) simulation model, (b) actual target.

Examining Fig. 5, a considerable amount of ripple can be observed in the experimental data when compared to the smooth data obtained by the noise-free simulation data. A good agreement however is observed between both results in terms of time of arrival (The first peak), which forms the basis of the suggested reconstruction approach. Later parts of the signals show a relative trend of agreement between the recordings, but are not fully matching. These mismatches can be attributed to the experimental parameters that are not considered in the simulation, including and not limited to floor reflections, reflection from other lab equipment, and individual characteristics of each antenna. It is also important to recall that the simulation is performed in a 2D space. However, the later parts of the signals are not of substantial importance in this regard since full wave inversion and quantitative mapping is not considered in the reconstruction approach [17].

Following the results obtained in the first setup, the experiment is repeated again using the test dummy. The dummy was placed behind the wall barrier with the closest point (hand) 15 cm away. The hand is moved towards the barrier as can be observed in Fig 6(a, b). Figure 6 (c) shows the reconstructed image. Examining this figure, an intersection point of the ellipses can be clearly seen integrating on the position of movement

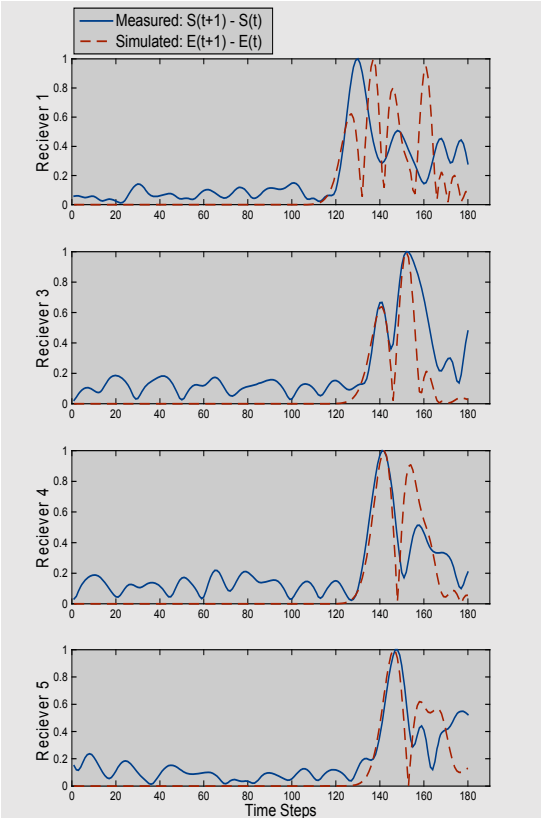

Figure 5 : Simulated and measured fields (normal magnitude) captured at receivers 1,3,4, and 5 due to to the excitation of transmitter 2.

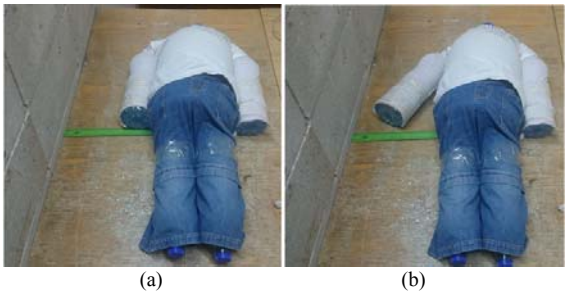

(a) (b)

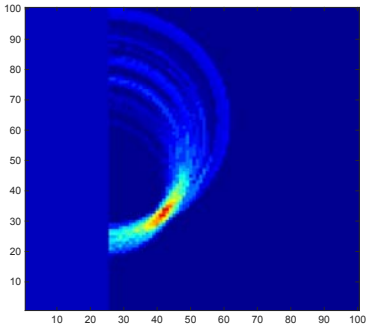

(c)

Fig 6: Detection of hand limb movement showing: (a) and (b) actual target before and after movement, and (c) the detected image

To investigate the effects of possible random rubble, the dummy was placed 30 cm away from the wall (nearest point), and a 20 cm thick concrete block was placed in the middle, can illustrated in Fig. 7(a). The experiment was repeated again, and corresponding data was recorded for an assumed leg movement, as illustrated in Fig. 7(b). Fig. 7(c) shows the reconstructed image.

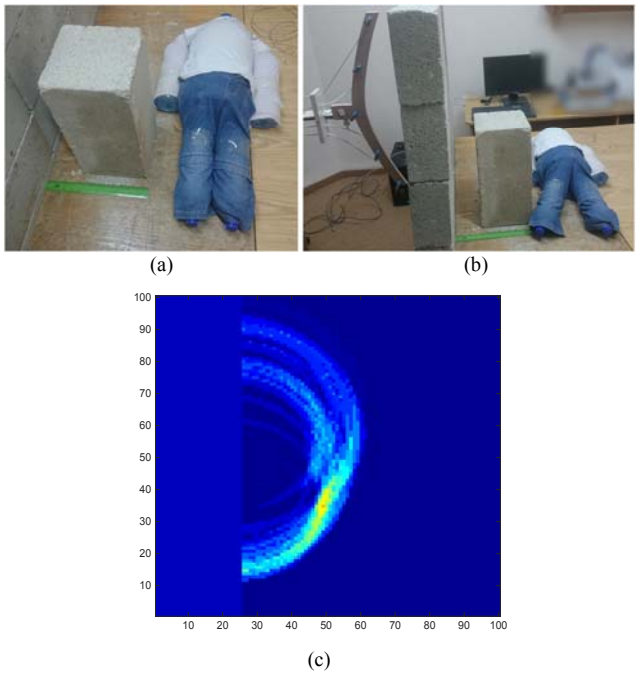

Fig 7: Detection of hand limb movement showing: (a) and (b) actual target before and after movement, and (c) the detected image

Examining the reconstructed result, it can be observed that the motion has been detected. However, and when compared to Fig. 6(c), the intersection of lines is more spread, highlighting an area rather than a point. As the target is displaced further away from the barrier, the ability to differentiate the TDOA from noise becomes more difficult, and consequently, failure of integration around a single point.

V. Conclusion

In this paper, a preliminary experimental setup was used to validate simulation data for through rubble detection. The results show a good agreement between experimental and simulation data. Furthermore, experimental data was used to validate the image reconstruction approach based on TDOA of UWB signals and multilateration reconstruction.

Unlike reconstructions based on simulation data, which showed the detection capability beyond 50 cm of solid concrete and breathing signs [15], the current experimental setup was capable of providing good results when the target was in close proximity with the wall barrier. However, successful detection was achieved at a 30 cm depth with random rubble obstructing the target. No priori or estimations were used for reconstruction. The current experimental setup validates the mathematical reconstruction approach. However, this setup requires modification to allow for deeper detection. Better and more directive antenna design, and isolation of the array from areas outside the scanning range. These enhancements are actively being studied at our lab, and are the focus of ongoing research.

Acknowledgment

This research is supported by AAUJ Scientific Research Council fund: SRC 2013/2014 (1).

References

[1] Y. K. Wang, L. Li, X. Y. Zhou, and T. J. Cui, "Supervised Automatic Detection of UWB Ground-Penetrating Radar Targets Using the Regression SSIM Measure," IEEE Geoscience and Remote Sensing Letters, vol. 13, pp. 621-625, 2016.

[2] T. F. Zanoon and M. Z. Abdullah, "Early stage breast cancer detection by means of time-domain ultra-wide band sensing," Measurement Science and Technology, vol. 22, p. 114016, 2011.

[3] T. S. Ralston, G. L. Charvat, and J. E. Peabody, "Real-time through-wall imaging using an ultrawideband multiple-input multiple-output (MIMO) phased array radar system," in Phased Array Systems and Technology (ARRAY), 2010 IEEE International Symposium on, 2010, pp. 551-558.

[4] M. G. Amin, Through-the-Wall Radar Imaging: CRC Press, 2016.

[5] E. J. Baranoski, "Through-wall imaging: Historical perspective and future directions," Journal of the Franklin Institute, vol. 345, pp. 556-569, 9// 2008.

[6] T. F. A. Zanoon and M. Z. Abduallah, "A hybrid image reconstruction approach for ultra-wide band microwave tomography featuring radar based and iterative methods," in 2014 IEEE International Conference on Imaging Systems and Techniques (IST) Proceedings, 2014, pp. 17-21.

[7] J. Laviada, A. Arboleya, L. F, x00F, G. pez, and F. Las-Heras, "Broadband Synthetic Aperture Scanning System for Three-Dimensional Through-the-Wall Inspection," IEEE Geoscience and Remote Sensing Letters, vol. 13, pp. 97-101, 2016.

[8] F. Soldovieri, R. Solimene, and R. Pierri, "A simple strategy to detect changes in through the wall imaging," Progress In Electromagnetics Research M, vol. 7, pp. 1-13, 2009.

[9] J. Moulton, S. Kassam, F. Ahmad, M. Amin, and K. Yemelyanov, "Target and change detection in synthetic aperture radar sensing of urban structures," in 2008 IEEE Radar Conference, 2008, pp. 1-6.

[10] K. Ranney, A. Martone, L. Nguyen, B. Stanton, M. Ressler, and e. al, "Recent MTI experiments using ARL's synchronous impulse reconstruction (SIRE) radar," in SPIE 6947, Radar Sensor Technology XII, 694708, Fl. USA, 2008.

[11] Y. Xu, S. Wu, C. Chen, J. Chen and G. Fang, "A Novel Method for Automatic Detection of Trapped Victims by Ultrawideband Radar," IEEE Transactions on Geoscience and Remote Sensing, vol. 50, no. 8, pp. 3132-3142, Aug. 2012.

[12] M. Donelli, "A rescue radar system for the detection of victims trapped under rubble based on the independent component analysis algorithm," Progress In Electromagnetics Research M, Vol. 19, 173-181, 2011.

[13] E. Zaikov, "UWB radar for detection and localization of trapped people," 11-th International Radar Symposium, Vilnius, 2010, pp. 1-4.

[14] A. Faize, A. Driouach, " Possibility of using GPR Radar to localize human bodies under the rubble caused by an earthquake," International Journal of Engineering Research and Applications, Vol. 2, Issue 2, , pp.284-286, 2012.

[15] T. F. A. Zanoon, "Disaster recovery and through rubble detection by means of quasi-real time UWB multilateration reconstruction," *2016 IEEE Asia-Pacific Conference on Applied Electromagnetics (APACE)*, Langkawi, 2016, pp. 358-363. doi: 10.1109/APACE.2016.7916460

[16] C. Thajudeen, A. Hoorfar, F. Ahmad, and T. Dogaru, "Measured complex permittivity of walls with different hydration levels and the effect on power estimation of twri target returns," Progress In Electromagnetics Research B, vol. 30, pp. 177-199,, 2011.

[17] T. F. Zanoon and M. Z. Abdullah, "Quantitative Imaging in the Time Domain Featuring Gradient Based Minimization and Broyden Updating," in *IEEE Microwave and Wireless Components Letters*, vol. 21, no. 11, pp. 628-630, Nov. 2011. doi: 10.1109/LMWC.2011.2168602